Measurement of Liver Volume by Emission Computed Tomography

Michael K. Kan and G. Bruce Hopkins

Scripps Memorial Hospital, La Jolla, California

In 22 volunteers without clinical or laboratory evidence of liver disease, liver volume was determined using single-photon emission computed tomography (ECT). This technique provided excellent object contrast between the liver and its surroundings and permitted calculation of liver volume without geometric assumptions about the liver's configuration. Reproducibility of results was satisfactory, with a root-mean-square error of less than 6% between duplicate measurements in 15 individuals. The volume measurements were validated by the use of phantoms.

The determination of liver size has been difficult by clinical estimation (*1–2*). Various radiographic methods have been used but these have not gained general acceptance and have been superseded by radionuclide and ultrasound studies (*3–5*). Even in radionuclide imaging, the determination of liver volume is difficult because of the myriad of possible liver configurations encountered clinically (*6*). We have explored the feasibility of liver-volume determination using emission computed tomography (ECT).

METHODS AND MATERIALS

Emission computed tomography of the liver and spleen were carried out in 22 normal volunteers. The subjects ranged in age from 19 to 54 yr and had no evidence of liver or systemic disease either by history, routine chemistry panel, or complete blood count performed just before imaging. Body weight and height were used to estimate body surface area, as shown in Table 1.

Each subject was given 5 mCi of Tc-99m sulfur colloid 20-30 min before imaging began, with the dose given intravenously in the hand or lower forearm, below the level of the spleen in the sitting position. Accidental extravasation at the antecubital fossa might cause errors in the reconstruction of the liver image.

A scintillation camera with large field of view and high-resolution low-energy parallel-hole collimator was used for all the studies. Routine views of the liver and spleen were recorded on transparent film and Polaroids for interpretation. Data for ECT were collected and analyzed on a minicomputer with 32K-word core memory and magnetic-disc storage. The subject sat on a pivoted bar stool with thin supporting back; during data collection he was rotated through 360° with 5.6° increments. Care was taken to ensure that both liver and spleen were within the view of the scintillation camera in all projections.

The basic arrangement of our ECT system was similar to that used by Budinger et al. (*7*) with the exception that the bar stool replaced their rotating platform. The spatial resolution of our system was at or slightly above 2 cm for body imaging. Phantom studies showed that the contrast and resolution of the ECT images were significantly better than in standard scintiphotos. For example, cold lesions simulated by placing 3-cm and 4-cm air-filled plastic spheres in various parts of the liver phantom were better delineated on the ECT images (Figs. 1–3). The liver phantom closely matched the shape of a normal human liver, with indentations representing the renal fossa and interlobular fissure. Its volume

514

TABLE 1. LIVER VOLUMES FOR 22 NORMAL VOLUNTEERS

Patient No.	Sex	Age	Height (cm)	Weight (kg)	Computed body surface* (sq. m)	Liver vol. (liters)	Ratio of Liver vol to body area (l/sq.m)	Ratio of Body wt. to liver vol. (kg/l)	Vertical height of liver† (cm)
1	M	22	175	70	1.85	1.392	0.752	50.2	12.0
2	F	54	167	58	1.66	1.373	0.827	42.2	14.3
3	F	27	152	47	1.41	1.036	0.734	45.3	12.5
4	F	28	172	61	1.72	1.622	0.943	37.6	16.1
5	F	29	154	49	1.46	1.288	0.882	38.0	15.3
6	F	50	168	57	1.65	1.517	0.919	37.5	19.3
7	F	47	151	46	1.39	1.171	0.842	39.2	12.7
8	F	31	175	58	1.70	1.294	0.761	44.8	12.5
9	M	36	172	56	1.67	1.322	0.791	42.3	10.0
10	F	27	165	61	1.67	1.236	0.740	49.3	14.2
11	M	20	179	72	1.90	1.900	1.000	37.8	15.1
12	M	21	182	80	2.02	1.864	0.922	42.9	12.8
13	F	26	177	61	1.76	1.425	0.809	42.8	12.1
14	M	31	172	74	1.88	1.661	0.883	44.5	9.6
15	M	19	175	61	1.74	1.655	0.951	36.8	13.2
16	M	24	160	52	1.52	1.448	0.952	35.9	12.5
17	M	19	190	83	2.11	1.932	0.915	42.9	15.1
18	F	36	162	49	1.51	1.495	0.990	32.7	14.3
19	M	26	185	78	2.02	1.740	0.861	44.8	15.0
20	M	42	185	90	2.15	1.694	0.787	53.1	10.3
21	M	30	170	69	1.80	1.671	0.928	41.2	15.8
22	F	25	167	55	1.62	1.303	0.804	42.2	13.3

*Body surface area was calculated from body height and weight by formula of DuBois and DuBois (12)

$$\text{Body surface} = \text{weight}^{0.425} \times \text{height}^{0.725} \times 0.007184$$
$$\text{(sq.m.)} \qquad \text{(kg)} \qquad \text{(cm)}$$

†Midway between xiphoid and right lateral border

was 1.6 l. It was imaged in a standard torso phantom (29 cm wide, 21 cm thick) filled with water to simulate the clinical situation. All standard scintigrams and ECT images were obtained with approximately one million scintillation events.

For the volunteer studies, the data collection time for each view was 20 sec, and a typical study contained five to ten million scintillation events from the total of 64 projections. Tomographic reconstruction was carried out by the filtered back-projection technique (8). Correction for photon attenuation was approximated by using geometric means of opposing projections (9). After reconstruction, a series of tomographic images at various levels was obtained (Fig. 4), with each tomographic slice 2 pixels thicks (about 1.2 cm). Usually 12 to 18 slices bracketed the entire liver. For image display, background noise was removed by 5-10% background suppression.

In order to test the reproducibility of the measurement as regards positioning and data analysis, 15 of the 22 volunteers underwent a second similar study about 30 min after the first, with a rest in between and complete repositioning. The two sets of data were analyzed independently initially, and the first set was reanalyzed later to assess the var-

iations introduced by delineation of the liver edge alone.

To evaluate the accuracy of volume measurements, 16 liver-shaped phantoms, from 500 to 3500 ml in size, were placed in a torso phantom filled with water and were imaged under conditions similar to those in the volunteer study. With the exception of a standard-sized liver phantom used in a contrast-resolution study as described earlier, all other phantoms were constructed from plastic bottles of various sizes. In order to simulate the liver shape, portions of the plastic bottle were removed and replaced by beeswax sheets. These sheets were pliable and could be reshaped or curved inward to simulate the posteroinferior wall of the liver. The sheets are reinforced by masking tape and sealed with melted beeswax.

For the calculation of liver volume, the surface area of each tomographic slice was first obtained by flagging the liver area with a light pen. An edge program available on the computer, was used to mark the liver's edge (Fig. 5). The liver volume in each slice was obtained by multiplying the surface area by the center-to-center distance between adjacent slices. The total liver volume was derived by summing the volumes of the slices. The images
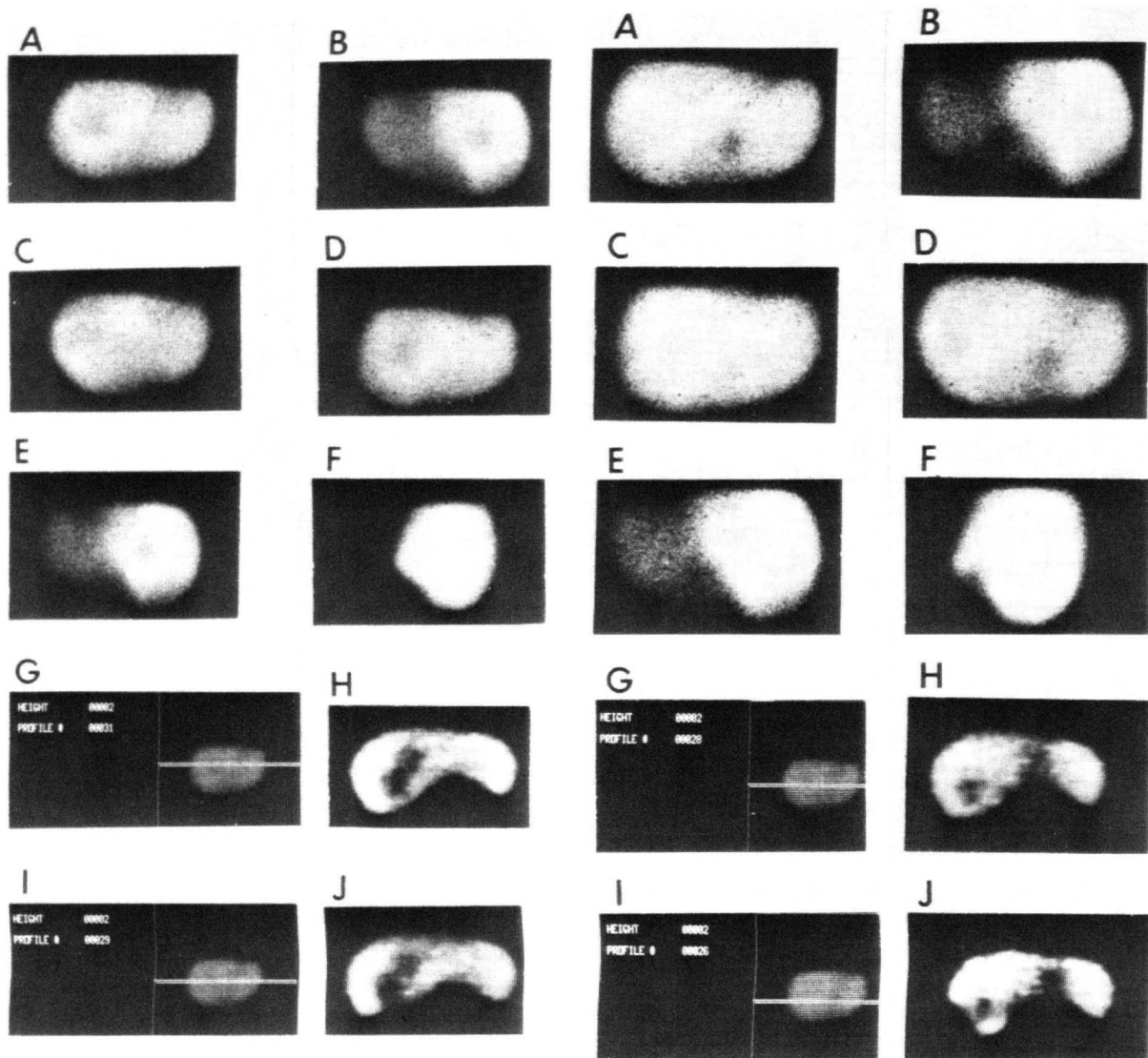
FIG. 1. Comparison of standard scintigrams and ECT images from liver phantom with simulated lesions. Standard scintigrams from anterior (A), posterior (B), left anterior oblique (C), right anterior oblique (D), and right posterior oblique (E) projections revealed a defect of relatively low contrast in right hepatic lobe. Right lateral projection (F) was within normal limits. ECT images (H, J) at two selected levels (G, I) correctly demonstrated two adjoining cold defects in right lobe. Cold lesions were simulated by a 3-cm sphere placed immediately anterior and medial to a 4-cm sphere in right lobe of liver phantom in exact locations shown by ECT images. The better contrast of cold defects on ECT images were not due to background subtraction or contrast enhancement. ECT images represent patient supine, with observer at his feet.

FIG. 2. Comparison of detectability of cold defects in liver phantom by standard scintigrams (A-F) and ECT images (H,J). Standard scintigrams (arranged as in Fig. 1) demonstrated cold defect simulated by a 3-cm sphere placed in quadrate lobe. Since the liver was relatively thin in this area, good contrast of this cold lesion was achieved on the standard scintigrams. Nevertheless, a second lesion simulated by a 4-cm sphere in posterior right lobe was not readily identified by standard scintigrams. ECT images (H,J) correctly identified both simulated lesions with good contrast.

were smoothed before applying the edge program.

RESULTS

In Fig. 6 the calculated volumes of the phantoms are plotted against the volumes actually measured by water displacement. The root-mean-square (rms) error was 7.2% and the correlation coefficient was good (r = 0.988) between the calculated and known volumes of the phantoms. The line of best fit was quite close to the 45° identity line. Using the regres-
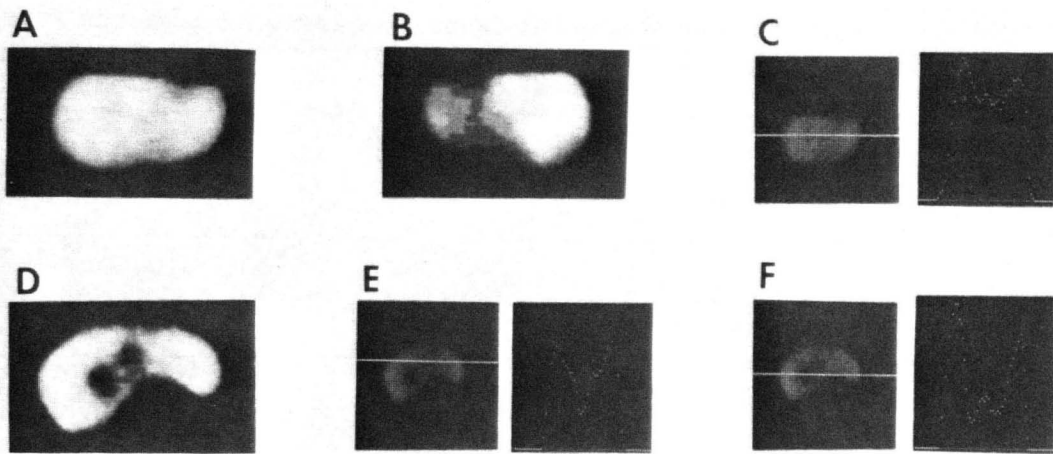
FIG. 3. Phantom study comparing contrast resolution between standard scintigrams (upper row) and ECT images (lower row). Two "cold" lesions were simulated by a 4-cm sphere in posteromedial part of right lobe and a 3-cm sphere placed medially and anterior to the 4-cm lesion. Cold lesions were not well delineated on standard scintigrams due to poor contrast, whereas ECT image at appropriate level (D) provided good delineation of both cold defects. Appreciation of exact location and relative sizes of lesions was possible only on ECT images. Comparison of profiles from standard scintigram (C) and from ECT image (E and F) revealed much better contrast of cold lesions in ECT image.

sion equation derived from the phantom study, the liver volumes of the volunteers and patients were computed and are summarized in Tables 1 and 2. There was good reproducibility in the duplicate

FIG. 4. Selected tomographic images of liver from a normal volunteer. Right-hand images represent subject supine, with observer at his feet.

liver volume measurements with a rms error of 5.4% between the two sets of data (Table 3). Repeat analysis of the first set of data revealed a rms error of 5.2%, which primarily represents the variations in delineation of the liver edge. There was poor correlation (r = 0.192) between the liver volume and the liver height measured midway between the xiphoid and the lateral border of the liver.

DISCUSSION

Our results for liver volumes of normal volunteers correlate well with data from the literature (13,14). DeLand and North (15) find that the expected normal liver mass for individuals with var-
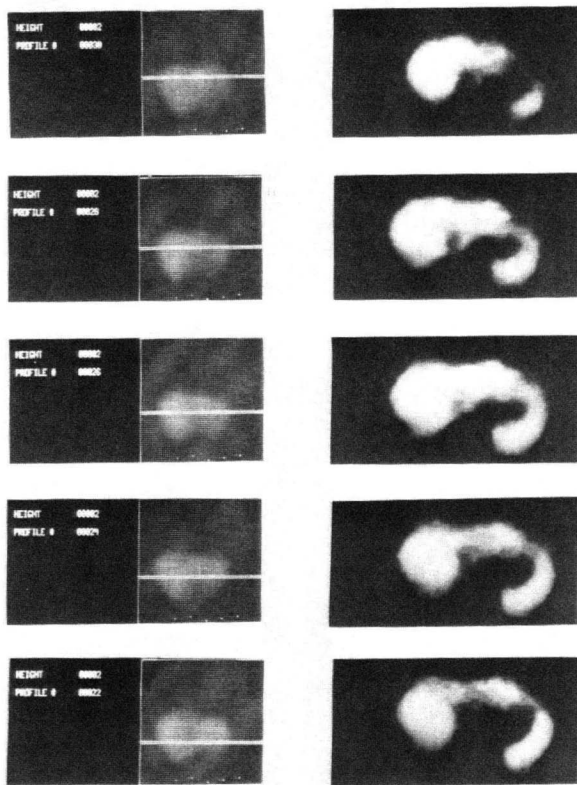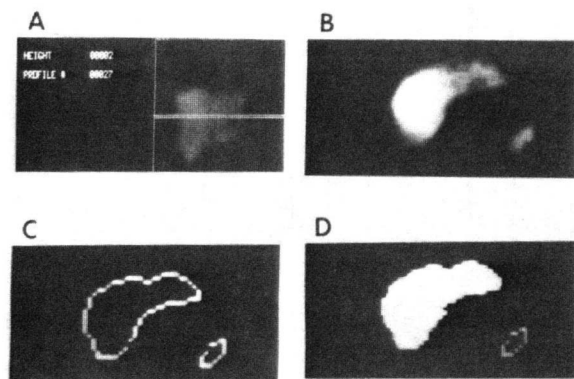

FIG. 5. Example of volume calculation for one tomographic slice of liver. Outline of liver can be identified by an edge program (C) and enclosed area is flagged by light pen (D). Volume of tomographic slice is obtained by multiplying area by center-to-center distance between adjacent slices. Total liver volume is sum of slice volumes.

TABLE 2. VARIOUS ESTIMATES OF ADULT LIVER WEIGHT

Series	Range (kg)	Mean (kg)	Ratio of body wt to liver wt
Popper & Schaffner (10)	1.4–1.6 (male) 1.2–1.4 (female)	NA	50
Goss (11)	1.4–1.6 (male) 1.2–1.4 (female)	NA	39
Gardner et al. (13)	1.0–3.0	NA	NA
Anson (14)	NA	1.69 (male) 1.40 (female)	NA
Current study	1.3–1.9 (male) 1.0–1.6 (female)	1.66 (male) 1.34 (female)	42

TABLE 3. DUPLICATE LIVER-VOLUME MEASUREMENTS IN 15 NORMAL VOLUNTEERS*

Patient No.	First measurement (liters)	Second measurement (liters)	% Difference $100\frac{(2)-(1)}{(1)}$
1	1.452	1.332	−8.2
2	1.313	1.434	+9.2
3	1.019	1.053	+3.3
4	1.567	1.677	+7.0
5	1.313	1.263	−3.8
6	1.523	1.511	−0.7
7	1.203	1.139	−5.3
8	1.360	1.229	−9.6
9	1.358	1.286	−5.3
10	1.206	1.266	+4.9
11	1.871	1.929	+3.0
12	1.818	1.910	+5.0
13	1.437	1.413	−1.6
14	1.649	1.673	+1.4
15	1.680	1.630	−2.9

* Second measurement (Y) was related to first (X) by Y = 1.07X − 0.11. Root-mean-square difference was 5.4%.

ious body surface areas can be derived using the equation Y = 1.02 X − 0.22, where Y = liver weight in Kg and X = computed body surface area in square meters. Our data agree well with the values derived from the above equation (Table 4). The good reproducibility between duplicate measurements suggests that variations in positioning do not significantly affect the results.

Liver volumes can be indirectly determined from the anterior and right lateral views of radionuclide images, but not without certain geometric assumptions regarding the liver configuration. In a previous
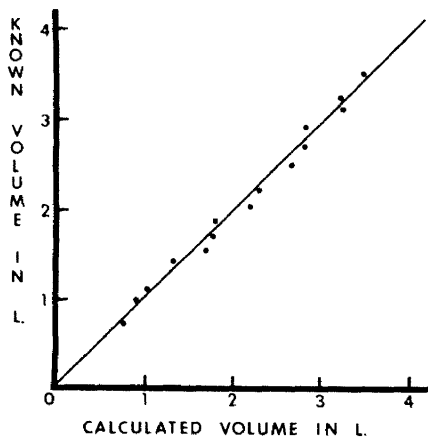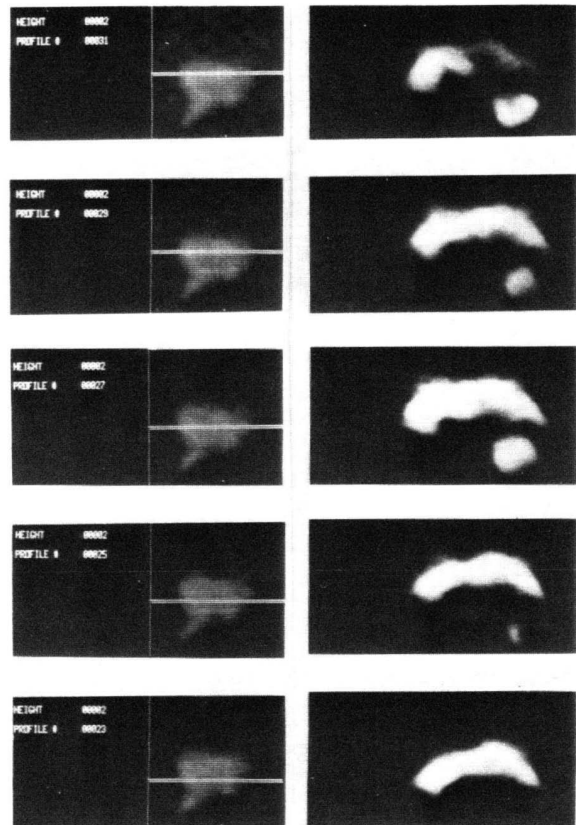

FIG. 6. Relationship between calculated and known volumes of phantoms. The regression equation is Y = 1.007 × + 0.014, where Y is known volume and X is calculated volume in liters. Coefficient of correlation, r = 0.988.

FIG. 7. Tomographic images from volunteer with short anteroposterior diameter of liver. Volume was 1.4 liters.

TABLE 4. COMPARISON OF LIVER VOLUMES IN NORMAL ADULTS WITH DIFFERENT BODY SURFACE AREAS

Range of body surface areas (sq. m)	No. of subjects	Mean body surface (sq. m)	Mean liver volume (liters) from current study	Expected liver wt. (kg) from eqn. of Deland and North (15)
1.30–1.59	5	1.45	1.29	1.25
1.60–1.89	12	1.72	1.45	1.53
1.90–2.19	5	2.04	1.82	1.86

report (16) the liver was arbitrarily considered to be composed of an ellipsoid (right lobe) and a paraboloid (left lobe). The advantage of our ECT approach is its complete independence of liver configuration, since no geometric assumption is necessary. Vertical height of the liver has also been used to estimate the liver size (17). The difficulty with this method lies in the great variation in the anteropos-

terior diameter of the liver among different individuals. In our series there is poor correlation between the liver volume and the vertical height of the liver measured midway between the xiphoid and the lateral border. For example, the tomographic images from a normal volunteer and from a patient with alcoholic cirrhosis are shown in Figs. 7 and 8. Although the vertical heights of the two livers are about the same, our calculated liver volume in the cirrhotic patient was twice that of the volunteer.

Although the current study is for measurement of liver volume, the same technique could be applied to other organs and for the sequential followup of patients with space-occupying lesions in the liver. One of the important factors that have made the ECT technique successful is the high object contrast it provides compared with conventional radionuclide or radiologic studies. This is an important consideration in comparing ECT and x-ray CT techniques (18) in clinical applications, since lesion detectability is dependent on object contrast as well as spatial resolution. Although x-ray CT provides excellent spatial resolution, the contrast of lesions in certain diseases may be so poor that it offsets the advantage in spatial resolution. By offering excellent object contrast and reasonable spatial resolution, the ECT technique would provide better delineation of the lesions in such cases. In liver-volume computation, accurate delineation of the liver boundaries is necessary by the current ECT technique. This is influenced by the spatial and contrast resolutions of the system used. In clinical situations where there is poor object contrast in the liver due to liver failure, the current technique will not perform well.

In our experience, the most important technical factor in ensuring a good study is accurate alignment of the rotating chair in front of the camera, since slight displacement would greatly degrade the final images. In addition, the patient should be positioned so that neither liver nor spleen will fall outside the view of the scintillation camera in any of the 64 projections. This is usually not a problem with the large field-of-view scintillation cameras.

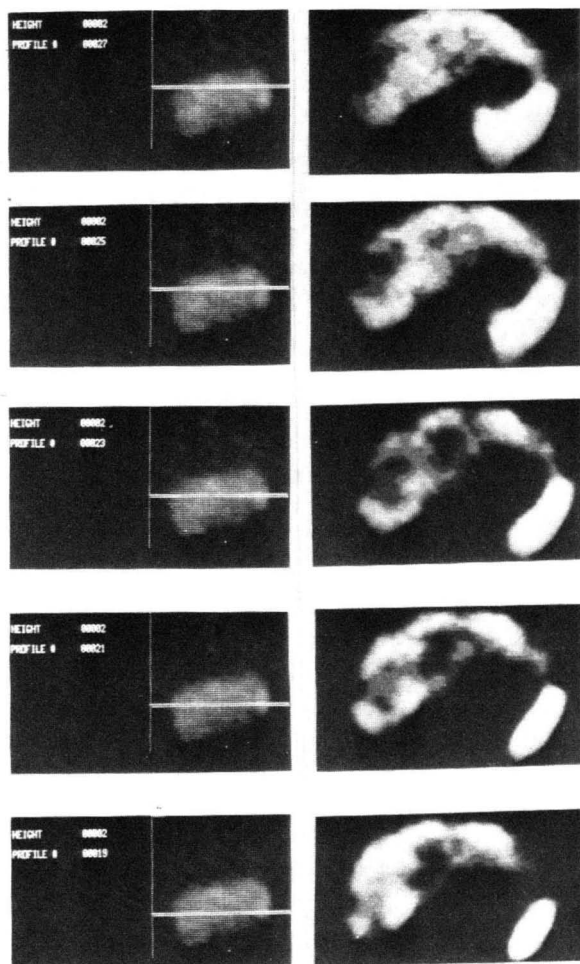Note that our method of attenuation correction using geometric means of opposing rays is not

FIG. 8. Tomographic liver images from patient with alcoholic cirrhosis. Although vertical height of liver was approximately the same as for case in Fig. 4, liver volume was twice as large (2.8 liters) due to diffuse enlargement of liver with increase in all diameters.

exact. However, it has not been a disadvantage for the current application since a great portion of the liver boundary is located close to the body surface and there is a high contrast ratio of radioactivity between the liver and its surroundings. It has been pointed out recently that tomographic cross sections of the abdomen show little changes in qualitative characteristics with or without photon-attenuation correction (19). For quantitative measurement of radioactivity within the liver, a more elaborate photon-attenuation correction scheme is desirable (20).

Since our method of liver-volume measurement uses single-photon emission tomography with an Anger camera, it can be implemented relatively easily in many laboratories. Apart from a rotating chair, a computer is required for data acquisition and tomographic reconstruction. For considerations of speed we have chosen the filtered backprojection technique (8) and a 64 × 64 matrix for reconstruction. Our system at present is not equipped with a hardware floating-point processor and multiply-divide unit; thus tomographic reconstruction took approximately 14 min per slice. The processing time should be reduced significantly by the addition of these hardware options.

REFERENCES

1. FLISCHNER FG, SAYEGH V: Assessment of size of liver: Roentgenologic consideration. N Engl J Med 259: 271-274, 1958

2. NIMEH W: New method for determination of size of the liver and spleen. Am J Gastroenterol 23: 147-156, 1955

3. WALK L: Roentgenologic determination of the liver volume. Acta Radiol 55: 49-56, 1961

4. FRIEDELL HL, MACINTYRE WJ, REJALI AM: A method for the visualization of the configuration and structure of the liver. Am J Roentgenol 77: 455-470, 1957

5. MCNULTY JG: Radiology of the Liver. Philadelphia, W B Saunders Co., 1977, p 30

6. MCAFEE JG, AUSE RG, WAGNER HN JR: Diagnostic value of scintillation scanning of the liver. Arch Intern Med 116: 95-110, 1965

7. BUDINGER TF, GULLBERG GT: Three-dimensional reconstruction in Nuclear Medicine emission imaging. IEEE Trans Nucl Sci 21: 2-20, 1974

8. BROOKS RA, DICHIRO G: Principles of computer assisted tomography (CAT) in radiographic and radioisotopic imaging. Phys Med Biol 21: 689-732, 1976

9. JASZCZAK RJ, MURPHY PH, HUARD D, et al: Radionuclide emission computed tomography of the head with Tc-99m and a scintillation camera. J Nucl Med 18: 373-380, 1977

10. POPPER H, SCHAFFNER F: Liver: Structure and Function. New York, Blakiston, 1957, p 163

11. GOSS CM: Gray's Anatomy, 29th ed. Philadelphia, Lea & Feibiger, 1973, pp 1245-1246

12. DUBOIS D, DUBOIS EF: A formula to estimate the approximate surface area if height and weight be known. Arch Intern Med 17: 863-871, 1916

13. GARDNER E, GRAY DJ, O]RAHILLY R: Anatomy, 4th ed. Philadelphia, W B Saunders Co., 1975, p 394

14. ANSON BJ: Morris' Human Anatomy, 12th ed. New York, McGraw-Hill, 1966, p 92

15. DELAND FH, NORTH WA: Relationship between liver size and body size. Radiology 91: 1195-1198, 1968

16. ROLLO FD, DELAND FH: The determination of liver mass from radionuclide images. Radiology 91 : 1191-1194, 1968

17. ROSENFELD AT, SCHNEIDER PB: Rapid evaluation of hepatic size on radioisotope scan. J Nucl Med 15: 237-240, 1974

18. PHELPS ME: Emission computed tomography. Semin Nucl Med 7: 337-365, 1977

19. MURPHY P, BURDINE J, MOORE M, et al: Single photon emission computed tomography (ECT) of the body. J Nucl Med 19: 683, 1978 (abst)

20. CHANG L: A method for attenuation correction in radionuclide computed tomography. IEEE Trans Nucl Sci 25: 638-642, 1978